Three pulse photon echo studies of nondipolar solvation: Comparison with a viscoelastic model

Delmar S. Larsen, Kaoru Ohta, and Graham R. Fleming

Citation: The Journal of Chemical Physics **111**, 8970 (1999); doi: 10.1063/1.480240
View online: http://dx.doi.org/10.1063/1.480240
View Table of Contents: http://scitation.aip.org/content/aip/journal/jcp/111/19?ver=pdfcov
Published by the AIP Publishing

Three pulse photon echo studies of nondipolar solvation: Comparison with a viscoelastic model

Delmar S. Larsen, Kaoru Ohta, and Graham R. Fleming
Department of Chemistry, University of California, Berkeley, Berkeley, California 94720-1460 and Physical Biosciences Division, Lawrence Berkeley National Laboratory, Berkeley, California 94720-1460

(Received 26 May 1999; accepted 23 August 1999)

Three pulse stimulated photon echo peak shift (3PEPS) measurements were used to probe the solvation of a quadrupolar solute in three room temperature nondipolar solvents; benzene, CCl_4, and CS_2, and the results were compared with those for two polar solvents, methanol and acetonitrile, and one weakly polar solvent, toluene. Our data reveal three distinct solvent dynamical time scales; a sub-100 fs ultrafast component attributed to inertial motions, a slow ($\sim$2–3 ps) component attributed to structural relaxation, and an intermediate time scale ($\sim$600 fs) of uncertain origin. The six solvents were chosen to reflect a range of possible interactions, but exhibit similar dynamics, suggesting that similar mechanisms may be at work or that different mechanisms may exist, but occur on similar time scales. A viscoelastic continuum solvation model proposed to describe nonpolar solvation [J. Phys. Chem. A **102**, 17 (1998)] was used for a preliminary analysis of our data. © *1999 American Institute of Physics.* [S0021-9606(99)50643-0]

I. INTRODUCTION

The time scales and mechanisms of polar solvation dynamics have been extensively studied both experimentally[1–10] and theoretically.[11–21] The basic mechanisms at work are broadly understood, and quantitative prediction of experimental data is possible when adequate dielectric data are available for a particular solvent.[13,22–28] The situation is quite different for nonpolar solvation where, with the notable exception of the work of Berg and co-workers,[29–33] few experimental studies exist and the feedback between theory and experiment that has been so productive for polar solvation has not yet been achieved for nonpolar systems.

There are a number of reasons why nonpolar or more generally nondipolar, solvation is of significance. Nonpolar systems refer to systems that interact via weak nonelectrostatic forces, e.g., dispersive and repulsive interactions, whereas nondipolar systems include higher electrostatic multipole (e.g., quadrupole or octupole) moments in addition to the nonpolar interactions. First, there is no obvious method to extract the dynamical time scales in nondipolar liquids from existing frequency domain data such as dielectric relaxation measurements. Second, the assumptions that greatly simplify the understanding of dipolar solvation, linear response[34–36] and the relative insensitivity of the time scales to the specific nature of the probe molecule may not hold for nonpolar or nondipolar solvation.[3,37,38] In other words, the short-range nature of the interactions implies that the molecular properties of the solvent–solute combination play a more important role in the solvation dynamics of nondipolar systems than in the dipolar case. Finally, an understanding of nondipolar solvation will have important implications for our understanding of mechanical or collisional friction in chemical dynamics.[39,40] A few specific examples are the connection between nonpolar solvation and the rates of vibrational energy relaxation and dephasing discussed by Stratt and co-workers,[40–42] and Bagchi and co-workers.[43,44]

In our study, the solvation of *N*,*N*, bis-dimethylphenyl 2,4,6,8, perylenetetracarbonyl diamide (PERY) in both nondipolar and dipolar solvents is investigated. In contrast to the probes used in many other solvation studies, our probe molecule, PERY (Fig. 1), is both nonionic and nondipolar. Due to PERY's D_{2h} symmetry, it lacks a permanent dipole moment in both the ground and excited states making the quadrupolar moment the next nonzero electrostatic moment. Semiclassical, molecular orbital calculations show that PERY's frontier orbitals lie predominately on the perylene base skeleton,[45] suggesting that the peripheral moieties may not contribute greatly to the solvation originating from electrostatic interactions. PERY is moderately soluble in both polar and nondipolar solvents with typical Stokes shift values ranging from $\sim$200 cm^{-1} in nondipolar solvents to $\sim$600 cm^{-1} in more polar solvents. These small Stokes shifts mean that, in contrast to typical polar solutes in polar solvents, the spectrum is characterized by a well resolved, discrete ''progression'' in high frequency modes, although it should be noted that these often correspond to combination bands rather than simple progressions in a single mode. This simpler vibrational structure, in addition to weak solute–solvent coupling, suggests that contributions from vibrational wave packets are likely to produce strong modulations in nonlinear spectroscopic data such as those observed in 3PEPS measurements. Such large amplitude modulations of the signal can complicate the extraction of the underlying solvation behavior. However we show that with our data, the beat patterns provide strong evidence for the existence of particular time scales during the lifetime of the vibrational wave packet.

Previously, time resolved florescence Stokes shift (TRFSS), hole burning, and photon echo measurements have been used to study nondipolar solvation. Reynolds *et al.* observed a distinct similarity between polar and nondipolar solvation dynamics using TRFSS measurements.[1] Berg and co-

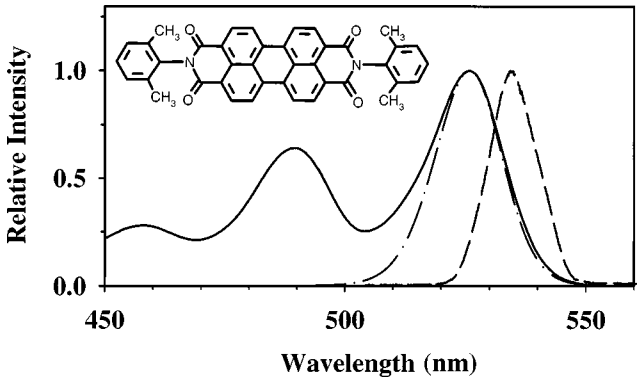

FIG. 1. Experimental absorption profile of PERY in benzene (solid line) along with the laser pulse spectrum (dashed line) and simulated absorption spectrum (dotted–dashed line). The simulated absorption spectrum was calculated with the parameters in Table II.

workers performed time-resolved hole burning measurements on dimethyl-*s*-tetrazine dissolved in *n*-butyl benzene at low temperatures,[29–33] and Fayer and co-workers measured two pulse photon echo decays from diphenyl acetylene dissolved in cyclohexane and 2-methyl pentane.[46] In this study, we measured three pulse stimulated photon echo peak shift (3PEPS) for PERY in three nondipolar solvents: benzene, CCl_4, and CS_2; one weakly polar solvent: toluene; and two strongly polar solvents: methanol and acetonitrile, all at room temperature. 3PEPS measurements have been used successfully to study polar solvation dynamics,[6–10,47] polymer glasses over a wide temperature range,[48–50] and protein dynamics.[51–53] Our study extends this technique to nondipolar solutions.

The 3PEPS technique is an ideal method of studying nondipolar room temperature systems. Unlike TRFSS measurements, which are limited to studying systems with strong coupling (Stokes shift >500 cm^{-1}), the ability of 3PEPS measurements to characterize solvation dynamics actually improves with more weakly coupled systems such as those studied here (Stokes shift ~ 300 cm^{-1}). In addition, the 3PEPS technique can measure a wide range of dynamical time scales from tens of femtoseconds to hundreds of picoseconds with subpulse (<40 fs) resolution.

II. EXPERIMENT

The details of the three pulse echo peak shift (3PEPS) measurement have been given elsewhere.[10,21,54] The 3PEPS data were collected using a commercial system consisting of a Ti:Sapphire laser (Coherent Mira Seed) pumped with a large frame Ar^+ ion laser (Coherent INNOVA 400). The resulting 76 MHz train of ~ 50 fs pulses, centered at 790 nm are stretched by a grating expander before seeding a regenerative amplifier (Coherent RegA 9050). The amplified pulses are then compressed and with an optical parametric amplifier (Coherent OPA 9450) used to create 530 nm pulses.[55,56] The pulse width was estimated to be near transform limited at 42 fs FWHM. Autocorrelations were measured with a 0.25 mm thick KDP crystal located at the sample position. Excitation to the red of the absorption maximum (Fig. 1) helps to minimize possible contributions of vibrational cooling to the signal.

TABLE I. Summary of solvent properties.

Solvent	(D)	$\langle Q \rangle$[a]	η[b]	ρ(g/cm^3)	Γ_{abs}[c]	ν_{abs}[c] (10^3)	$\Delta\nu$[d]	2λ[e]
CCl_4	0	0	0.97	1.5948	543	19.20	207	286
CS_2	0	1.18	0.33	1.2632	629	18.79	298	362
Benzene	0	8.35	0.65	0.8765	630	19.03	337	420
Toluene	0.3	7.92	0.59	0.8669	673	19.96	373	340
Acetonitrile	3.5	2.49	0.34	0.7857	673	19.19	364	294
Methanol	1.7	4.13	0.55	0.7914	1160	19.17	513	695

[a]The effective axial quadrupoles are used to quantify the magnitude of the quadrupole tensor and were calculated via *ab initio* methods in Ref. 1.
[b]Viscosities (20 °C) were taken from tabulations in Ref. 76 and are given in units of cP.
[c]Both bandwidth Γ (FWHM) and center frequencies ν_{abs} were measured from the first vibronic band of the absorption manifold.
[d]The Stokes shift is defined as the difference in energy between the lowest energy maximum in the fluorescence spectra and the highest energy maximum in the electronic absorption spectra. Dipole and average quadrupole moments were taken from Ref. 1. Densities are given at 20 °C and at 1 atm (Ref. 76).
[e]The Stokes shift values, 2λ, are obtained from the simulations results in Table II. The units for the spectral properties and the Stokes shift values are in cm^{-1}.

The experimental setup is similar in design to that used in previous 3PEPS measurements.[10,50,54] The parametrically amplified pulses are separated into three beams with equal pulse energies (5 nJ/pulse). Two of the three beams follow variable length paths enabling us to control the timing of the pulse interactions in the sample. All three beams are then focused near colinearly through a 20 cm singlet quartz lens into a 100 μm quartz flow cell where the sample was pumped with a flow rate of 30 mℓ/min to minimize thermal effects. We measured echo signals in an inverted triangle geometry at the phase-matching directions; $\mathbf{k_1}-\mathbf{k_2}+\mathbf{k_3}$ and $-\mathbf{k_1}+\mathbf{k_2}+\mathbf{k_3}$, where $\mathbf{k_1}$, $\mathbf{k_2}$, and $\mathbf{k_3}$ are the wave vectors of the first, second, and third pulses, respectively. The collection of the integrated echo signals in both directions allows us to measure the peak shift to a high precision.[10]

Both PERY and HPLC quality solvents were purchased from Aldrich. Prior to experimental use, PERY was dissolved and filtered to remove insoluble impurities. The solvents were used as received. All measurements were made at room temperature (20.5 °C±0.5 °C). Sample concentrations were kept low (0.08–0.12 O.D. in a 100 μm cell) to reduce the possibility of aggregation. A linear dependence of the signal on concentration was observed. To reduce possible solute-solute interactions, we keep the PERY concentration at a minimum.

III. RESULTS

We measured the 3PEPS signal in six solvents. Three are nondipolar (CS_2, CCl_4, and benzene), two are polar (acetonitrile and methanol), and one is weakly polar (toluene). These solvents were selected to represent a range of possible interactions (both solvent–solvent as well as solute-solvent) that may contribute to the experimental 3PEPS signal. Table I displays some of the more important characteristics of the

solvents, including their electrostatic properties (e.g., dipole and average quadrupole moments) and physical properties.[57]

The absorption spectrum for PERY in benzene is displayed in Fig. 1 and shows a striking similarity to the spectrum of the base structural component, perylene.[58,59] The spectra display the well resolved, narrow vibronic bands expected from the small solvent coupling of PERY systems. The small spectral shifts ($\sim$700 cm^{-1}) of the peaks indicate a weakly interacting, nonpolar transition. In contrast to the weakly coupled, nondipolar solvents, PERY's absorption spectra in dipolar solvents (Table I) are broader, indicating an increased solvent coupling. In methanol, the broadening is large enough (twice as broad as CCl_4) to partially obscure the underlying vibronic structure. In all solvents except methanol, PERY's emission spectrum is a near mirror image of the absorption profile, suggesting little or no excited-state intramolecular dynamics or solvent-dependent change in electronic structure. In contrast with the other solvents, the fluorescence spectrum of PERY in methanol demonstrates a marked change in intensity of the vibronic peaks, where emission at the second higher energy vibronic peak is approximately 20% greater than the first peak. The emission spectra of PERY in longer chain alcohols are nearly mirror images of the corresponding absorption spectra. Unlike some other solvation probes,[1] PERY is inert to highly reactive solvents like CCl_4. The significant breaking of the mirror-image symmetry between the absorption and fluorescence spectra in methanol suggests that the hydrogen bond interactions between the carbonyl groups on PERY and the hydroxyl groups on methanol may lead to altered line shapes. The altered emission spectrum of PERY in methanol implies that the Stokes shift shown for methanol in Table I therefore does not accurately represent the energetics of this system, i.e., the magnitude of the reorganization energy. In simulating the 3PEPS signal for methanol, we do not limit the total reorganization energy to the value suggested by the Stokes shift. The absorption spectra of the samples were checked before and after data collection, and the lack of an observable change suggests that little or no solute photodegradation or undesired chemical reactions occurred during the measurement.

To identify the peak shift, the integrated photon echo profiles are plotted against the coherence time, τ, at fixed population times, T. Typical integrated echo profiles for three population times (0 ps, 1 ps, and 70 ps) for the benzene solution are shown in Fig. 2. In previous studies of dipolar solutes in polar solvents, the photon echo profiles were fit well with Gaussian functions and the 3PEPS decay was constructed by measuring the span between the fit maxima. In contrast, our echo profiles display a distinct asymmetry that Gaussian functions cannot reproduce at small population times ($T<50$ fs). This asymmetry may arise from the slower dephasing time scales expected in weakly coupled systems,[60] in contrast to the fast dephasing typically found in polar solute/solvent systems where echo widths are insensitive to the population period. To account for this asymmetry, we fit the short population time profiles to cubic polynomials as described by de Boeij *et al.*[7] Fitting with polynomials instead of Gaussian functions increases the calculated peak shift by as much as 3 fs for population times less than 50 fs and yields equivalent results at longer times.

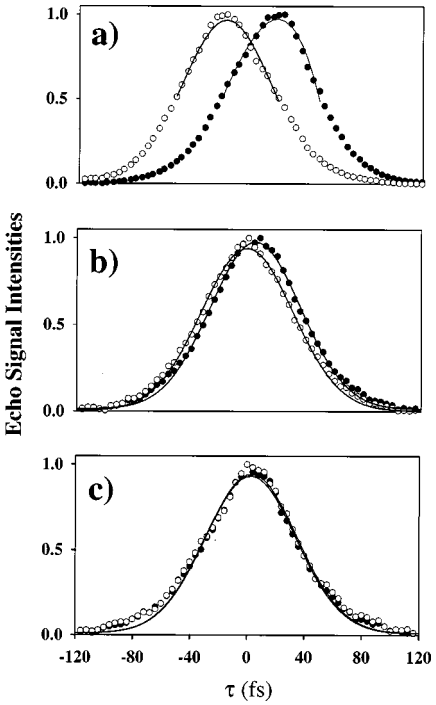

FIG. 2. Integrated photon echo profiles for PERY in benzene in the two phase matching directions $-\mathbf{k_1}+\mathbf{k_2}+\mathbf{k_3}$ (filled circles) and $\mathbf{k_1}-\mathbf{k_2}+\mathbf{k_3}$ (open circles) are displayed with fits (solid lines) used to calculated peak shift for fixed population times. (a) $T=0$ fs. (b) $T=1$ ps. (c) $T=70$ ps. Peak shift values are 19 fs, 3 fs, and 0.5 fs, respectively. Echo profiles are fit with cubic polynomials (see the text for details) at short times and with Gaussian functions at longer times.

Fayer *et al.* measured ultraviolet two-pulse photon echo (2PE) decays of nonpolar diphenyl acetylene dissolved in cyclohexane and 2-methyl pentane.[46] They observed a significant contribution of nonresonant signal, originating from the bulk solvent, superimposed on the resonant signal from the probe molecules. The nonresonant signals obscured the desired resonant signal; thus, the authors used the novel approach of investigating the pulse duration dependence of the echo profiles to measure the dephasing time, T_2, of the system. In the UV photon echo experiment, the excitation wavelength approached the one photon resonance and was within two-photon resonance of the solvent and hence the nonresonant signal was strongly enhanced. We encountered a similar difficulty. With suitable experimental sensitivity, a nonresonant, homodyned-detected, transient grating optical Kerr effect (TG-OKE) signal originating predominately from solvent molecules can be observed in the *same phase-matching direction* as the resonant photon echoes signals. With five of the six solvents studied here, this TG-OKE signal is negligible compared to the intensity of photon echo signal. Conversely, for PERY dissolved in CS_2, the highly polarizable solvent molecules contribute significantly to the total observed signal at population times less than 600 fs. This leads to distortion of the peak shift profiles, giving smaller peak shifts than would arise from PERY alone. The initial peak shifts measured in all other weakly coupled nondipolar solvents are in the 18–20 fs range, while the initial peak shift

observed in CS_2 is 12 fs (even smaller than the initial 14 fs peak shift in the more strongly coupled methanol). The peak shift data collected during the period that the TG-OKE signal contributes appreciably (<600 fs) for CS_2 were not simulated. A scheme for identifying and separating the TG-OKE signal from the photon echo signal may be possible, but was not attempted in this study.

Figures 3 and 4 show 3PEPS data for PERY in the various solvents. The noticeably strong oscillations arising from the 139 cm^{-1} and 278 cm^{-1} modes are very striking and persist for several picoseconds. In the more strongly coupled systems, methanol and acetonitrile, the magnitude of these beats appear diminished, but careful investigation shows that their absolute magnitude does not change greatly, only their relative magnitude with respect to other dynamical solvation processes that dominate the signal (see Table II).

In addition to the short time components, the insets in Figs. 3 and 4 clearly illustrate the existence of slow (50–100 ps) long time components. The origin of these time scales is uncertain. One possibility is that these long-time components reflect the dynamics associated with solute reorientational motion, which we expect to occur on this time scale.[61] Observation of such solute rotational dynamics in 3PEPS studies would require the existence of even longer (>100 ps) solvation time scales. Similar long time components have recently been reported in 3PEPS studies of room temperature, low viscosity liquids suggesting that long time solvation components may exist.[7,62] The possibility of long-lived triplet states contributing to the signals was considered but rejected. Yang *et al.* showed for a three-level system with a long lived excited state, that even though the measured intensity of the 3PEPS signals is decreased when compared to a two-level system, the measured peak shift profiles will be nearly identical.[63] Other explanations such as intramolecular solute isomerization or excited state reactions are unlikely because of the highly rigid nature of the PERY molecule (Fig. 1) and its high photostability. Further studies, including viscosity and solvent dependence, are planned to probe the nature of these time scales. Fortunately, these long time dynamics do not interfere with the characterization of the shorter time scale dynamics.

In contrast to previous 3PEPS measurements,[10,54] we do not observe an ultrafast (6–10 fs) time scale originating from the rapid interference of coherently excited high frequency intramolecular modes. In our study, the longer pulse duration (42 fs FWHM) and the resolved spectrum allows reasonable selectivity in excitation. To resolve these fast intramolecular dynamics, shorter pulse would be needed. Aside from the lack of this ultrafast component, all the solvents show time scales similar to those observed in previous room temperature polar and nondipolar studies.[8,10,20,64,65] In all the solvents, we find a sub-200 fs, ultrafast component accounting for ~40%–60% of the solvent relaxation. Similar time scales have been observed in previous 3PEPS experiments on polar systems.[6–10,47] The agreement of the experimental data with the simulated 3PEPS signals varies from solvent to solvent and is noticeably poorer in the strongly polar solvents: methanol and acetonitrile, where the initial peak shift values are significantly overestimated. In CCl_4 (Fig. 3) and benzene (Fig. 4) our simulations agree with the experimental data at short times (even to 25 fs for benzene). We have observed this failure at short times before with polar solutes in polar solvents where the spectra are unresolved. In systems where we were able to study a large temperature range, the agreement at short population times has always been improved at

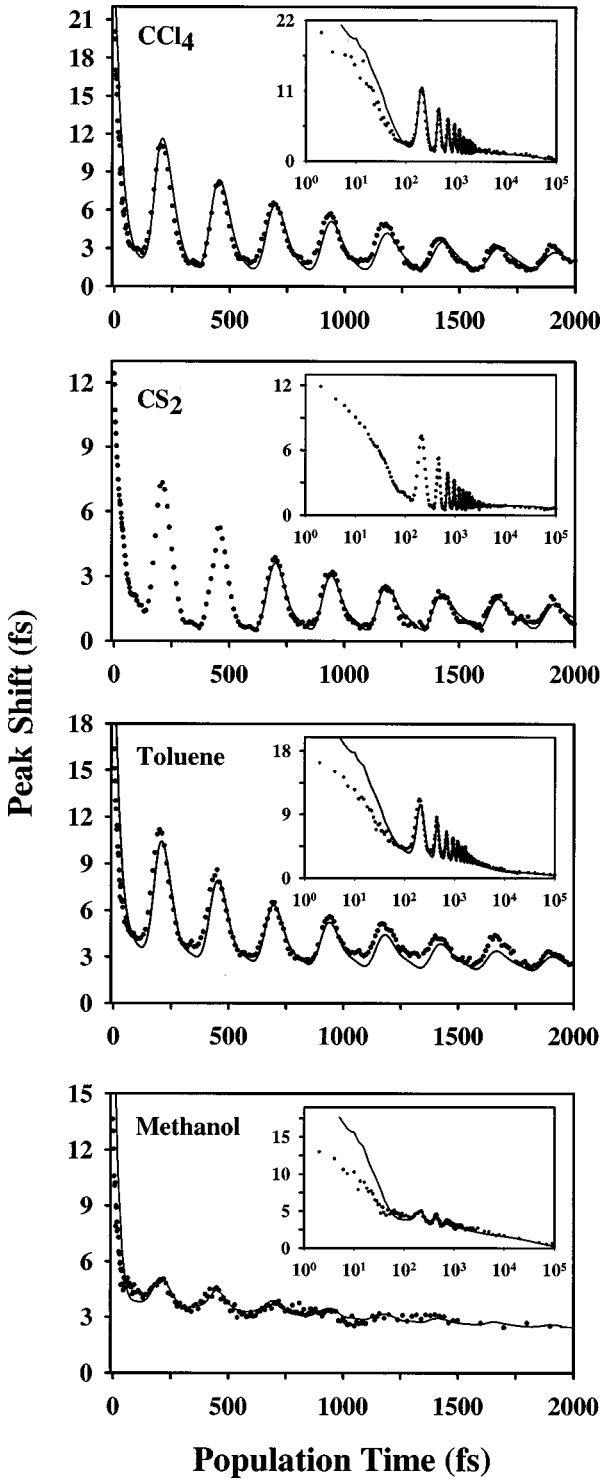

FIG. 3. Comparison of the experimental 3PEPS profiles (filled circles) and of best fit simulations (solid line) of PERY in four of the six studied solvents. The same comparison is displayed on a log scales in the insets. Simulations include a 42 fs pulse duration. Note that the panels do not share the same peak shift axis.

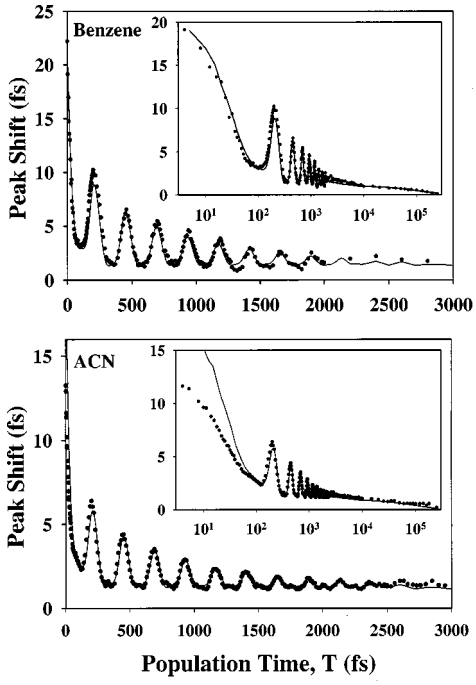

FIG. 4. (Upper panel) 3PEPS profile of PERY in benzene (filled circles) displayed with simulation (solid line) using parameters in Table II. The inset shows the same comparison extended to 250 ps on a log scale, and clearly shows the existence of a long time relaxation component. (lower panel) Same comparison of PERY in acetonitrile and simulation (Table II) with a similar inset. Simulations include a pulse duration of 42 fs FWHM.

low temperatures.[48,50] This suggests that we are not including a solvent dependent or thermal contribution to the line broadening correctly, for example, solvent-mediated intramolecular vibrational redistribution (IVR) or anharmonic spectral density effects. Future studies, including temperature dependent and spectrally resolved 3PEPS experiments, are planned to investigate the processes that contribute to the sub-100 fs relaxation in the peak shift curves.

All the solvents, with the exception of methanol and CS_2, also show relaxation behavior on two slower time scales ($\sim$650$\pm$200 fs and $\sim$2.5$\pm$0.5 ps) with solvent-dependent amplitudes. CS_2, commonly considered an anomaly in many comparative studies, relaxes within the first few picoseconds, while methanol lacks the subpicosecond time scale and decays on a longer time scale. We assume these relaxation time scales to be diffusional in nature and model them as exponential decays.

It might be assumed that the strong vibrational beats would compromise our ability to extract intermediate time scales; this is partially true. However, the presence of the persistent, large amplitude quantum beats enables us to both confirm the $\sim$650 fs components in our data and characterize some of the initial relaxation decays. In the absence of other dynamical processes, a quantum beat will oscillate symmetrically about the time axis, and the characteristic damping time for the beat can be observed on both the maxima and minima sides of the oscillation. In all of the solvents except methanol, the decay of the beat is noticeable only on the maxima side with the minima side being almost flat (Figs. 3 and 4), indicating the presence of an underlying time scale with a decay comparable to the damping time of the beat. In contrast with other solvents, the initial beat patterns in the 3PEPS profiles of acetonitrile and benzene demonstrate that their initial relaxation occurs more slowly than the other solvents. In these solvents, the first minimum is noticeably higher than the second, indicating that the initial solvent relaxation is occurring during this time scale.

In room temperature liquids, where a clear separation of solvent time scales may not exist, peak shift measurements

TABLE II. 3PEPS simulation results.

		Intramolecular contributions[a]		Intermolecular contributions			
Solvent		139 cm^{-1} vib.	278 cm^{-1} vib.	Solvent Gaussian	Solvent decay #1	Solvent decay #2	Long time component Relaxation decay
CCl_4	λ	45 cm^{-1}	15 cm^{-1}	45 cm^{-1}	20 cm^{-1}	10 cm^{-1}	8 cm^{-1}
	τ	860 fs	712 fs	80 fs	500 fs	2.0 ps	60 ps
CS_2	λ	27 cm^{-1}	9 cm^{-1}	70 cm^{-1}[b]	70 cm^{-1}	⋯	5 cm^{-1}
	τ	1100 fs	1100 fs	⋯	850 fs	⋯	200 ps
benzene	λ	45 cm^{-1}	15 cm^{-1}	50 cm^{-1}	30 cm^{-1}	60 cm^{-1}	10 cm^{-1}
	τ	820 fs	712 fs	150 fs	650 fs	2.2 ps	120 ps
toluene	λ	45 cm^{-1}	15 cm^{-1}	40 cm^{-1}	26 cm^{-1}	30 cm^{-1}	14 cm^{-1}
	τ	820 fs	712 fs	80 fs	650 fs	3.0 ps	120 ps
acetonitrile	λ	30 cm^{-1}	10 cm^{-1}	80 cm^{-1}	13 cm^{-1}	7.5 cm^{-1}	6.5 cm^{-1}
	τ	800 fs	750 fs	130 fs	500 fs	2.5 ps	50 ps
methanol	λ	28 cm^{-1}	9.5 cm^{-1}	150 cm^{-1}	⋯	70 cm^{-1}	90 cm^{-1}
	τ	820 fs	712 fs	60 fs	⋯	1.8 ps	80 ps

[a]Intramolecular vibrational contributions to the transition frequency correlation function, $M(t)$, were modeled as $\lambda_i \exp(t/\tau_i)\cos(\omega t+\phi_i)$ with a finite phase, ϕ_i, of 0.15 rad for the 139 cm^{-1} vibration and a zero phase for the 278 cm^{-1} vibration.

[b]The nonresonant signal from the CS_2 contributes significantly to observed resonant photon echo signal at times prior to $\sim$600 fs. Although shorter time scales cannot be resolved, the magnitude of the dynamical coupling in this solvent can be determined with confidence.

enable us to characterize the solvation time scales via an energy gap correlation function, $M(t)$, which represents, in the time domain, the fluctuations that modulate the energy gap of the probe molecule and lead to solvent relaxation.[66] In the high temperature limit, $M(t)$ is proportional to the solvation energy relaxation function, $S(t)$, that is directly measured in TRFSS and hole burning measurements. Even though the peak shift decay curves are correlated with $M(t)$, they do not directly measure $M(t)$.[21] Hence the direct interpretation of the 3PEPS data as the $M(t)$ will lead to erroneous conclusions. To extract the solvation solvation time scales in our data, we simulated both the measured 3PEPS data and absorption spectra. Simulation of the 3PEPS data requires the construction of a model $M(t)$ to represent the observed dynamics. We model the $M(t)$ relaxation function with the form,

$$M(t)=\lambda_g \exp[-(t/\tau_g)^2]+\sum_i \lambda_{\mathrm{sol},i} \exp[-(t/\tau_{\mathrm{sol},i})] + \sum_{i=1}^{2} \lambda_{\mathrm{vib},i} \exp[-(t/\tau_{\mathrm{vib},i})]\cos[\omega_{\mathrm{vib},i}t+\phi_{\mathrm{vib},i}] + \lambda_{\mathrm{long},i} \exp[-(t/\tau_{\mathrm{long},i})]. \quad (1)$$

The $M(t)$ functions can be separated into two components; a solute contribution and a solvation contribution. The solvation contribution is represented by the first two terms in Eq. (1), which includes a subhundred femtosecond ultrafast relaxation component that is commonly interpreted as inertial in origin[20] and we model as a Gaussian function with time constant, τ_g. Longer time solvation components, arising from diffusional or structural relaxation of the solvent, are modeled with exponential decays with corresponding time constants, τ_{sol}. Solute intramolecular vibrational dynamics are represented with the summation in Eq. (1). Intramolecular vibrational wave packet motions, observed as quantum beats in our data, are modeled with damped cosines with nonzero phases. The weakly damped, large amplitude vibrations in the data clearly indicate the presence of a nonzero phase for the 139 cm^{-1} oscillation. Brownian oscillators, commonly used to represent intramolecular vibrations in dynamical studies,[6] cannot model the quantum beats due to their inability to include phase information. The long time relaxation components of uncertain origin, were modeled as exponential decays with ~100 ps time constants, τ_{long}. This separation of $M(t)$ into solute and solvent components is not rigorous and is suspect in some cases (e.g., when intramolecular dynamics occur within the probe). Here, the separation is used only to help identify the primary nature of relaxation components.

We simulated our data as a two-level system coupled to a solvent bath of harmonic oscillators. The details of these simulations are published elsewhere,[10] but to capture the essence of the process we briefly describe it here. The simulation of the 3PEPS profiles requires the integration of a calculated response function (in our case calculated from the spin-boson model)[66] over all three pulse durations. The resulting bare echo signals are then integrated to generate the integrated echo profiles measured in the laboratory (Fig. 2). The peak shift is then obtained by measuring the maximum of the integrated echo profiles as a function of population time, T. At short times, where the pulses overlap (free-induction decay like) nonrephasing signals add to the rephasing signals, and further complicate the peak shift calculations. This complex procedure means that the final simulated 3PEPS profiles are not simple convolutions of underlying $M(t)$ functions with the pulse duration. As Figs. 1, 3, and 4 demonstrate, with the exception of the first 50 fs, we have successfully modeled both the 3PEPS signals and the absorption spectra of the studied systems.

Despite the disagreement between simulations and experimental data at very early times (<50 fs), we feel that the parameters of our simulations (Table II) accurately represent the time scales and relative magnitudes of the dynamics observed in our data. Even though some of the simulated time scales are similar to the region of poor fitting, the high precision and fine resolution of our data in conjunction with the analysis of the beat patterns (see Discussion) allow us to characterize both sub-200 fs and picosecond relaxation time scales with relatively small uncertainty. Possible origins for short time fits are discussed in the next section.

The modeling of the 3PEPS data should also generate the Stokes shift. The Stokes shift for a specific system is determined by $2\lambda_{\mathrm{tot}}$, where λ_{tot} is the sum of the reorganization energies of the components for respective solvent. As illustrated in Table I, the Stokes shifts obtained from simulations for many of the solvents, are quite similar to the values we obtain from experiment. Unfortunately, the comparison is not perfect in all solvents. One explanation for the observed discrepancies, is the underestimation the contributions of intramolecular modes (overdamped and nonimpulsively excited modes) that do not produce clearly resolved quantum beats. Ignoring such contributions to the peak shift necessitates an increased coupling of the intermolecular modes (solvent modes) to obtain agreement between the simulations and data. Additionally, as Table II demonstrates, the long time (>50 ps) relaxation component which is of uncertain origin, can contribute significantly to the total reorganization energy in certain solvents (e.g., methanol). This complicates the comparison between the Stokes shift values obtained via simulation and the measured values. In a previous peak shift study, Wiersma and co-workers[7] introduced long time components (~2 ns) into their simulations in such a way that they do not contribute to the observed Stokes shift values. As already noted, further experiments are required to clarify the origin of these long time components.

IV. DISCUSSION

The primary difficulty in comparing nonpolar or nondipolar solvation dynamics to theoretical models is the problem of obtaining the appropriate solvent time scales. In the case of polar systems, dielectric relaxation measurements can be used to predict solvation time scales, but since nondipolar systems exhibit weak macroscopic electrostatic responses, a different approach is required for these solvents. Berg,[29,67] Bagchi, and co-workers,[43,44] and Skinner and co-workers[68–70] have proposed theoretical models for strictly nonpolar dynamics. All three models appear somewhat dis-

tinct in their physical content, although they predict similar solvent dynamics. Both Bagchi and co-workers and Skinner and co-workers calculate the dynamics from the system's molecular properties and thus inherently include molecular level effects. In contrast, Berg treats the solvent as a viscoelastic (VE) continuum and calculates the nonpolar solvent response, $R(t)$, with frequency-dependent shear and longitudinal moduli.

As yet, we do not have analytical theories for the nondipolar solvation of a quadrupole, nor do we know the quadrupole moment of PERY (though this is certainly calculable). Thus, for an initial investigation of the time scales obtained in this work we have used the VE theory of Berg.[67] We use this theory as a method of calculating the expected time scales without presupposing that the mechanism of solvation behind the dynamics is purely that assumed by Berg. Later, we discuss the comparison of our data with molecular dynamics studies that give a microscopic description to nondipolar solvation.

A. Viscoelastic model

We begin by briefly outlining the viscoelastic model developed by Berg.[67] As noted above, the relevant dynamical response, $R(t)$, is characterized by the time-dependent shear and compression moduli, $G(t)$ and $K(t)$, respectively. The model is insensitive to whether the cavity bounded by the solute–solvent interface expands or contracts, but is quite sensitive to the coupling. K_s, of the solvent to the change in the cavity size. Once the appropriate viscoelastic equations of motion are solved, subject to initial and final boundary conditions, two time scales emerge; a fast coherent response associated with the time scales for acoustic longitudinal and transverse waves to traverse the dimensions of the solute and slower time scale that can be connected to the structural relaxation of the solvent.

Berg's VE response can be approximated as a sum of the phonon and the structural responses

$$R(t)\approx(1-f)R^{\mathrm{ph}}(t)+fR^{\mathrm{st}}(t), \tag{2}$$

where f is the relative contribution of the structural response to the total response and is sensitive to the infinite frequency shear modulus, G_∞, and the coupling parameter, K_s, which describes the resistance of the solvent to the cavity change.

When K_s is small, the phonon response can be expressed as a critically damped sinusoid with a corresponding time scale, τ_{ph} that is sensitive to the instantaneous values of the moduli and not to their full relaxation profiles. Since many solvents have similar high frequency values for their mechanical moduli, the fast dynamics of different solvents are predicted to have similar responses. Additionally, τ_{ph} is proportional to the solute radius, hence the VE model predicts slower dynamics from larger probe molecules. As we will show, this property introduces difficulty in applying the VE model to analyze solvation data measured with large probe molecules such as in our case.

Unlike the phonon response, the structural response is sensitive to the full relaxation profiles of the moduli. A common model used to describe the viscous relaxation of the moduli is the Maxwell model.[71] Within the Maxwell model, the shear modulus relaxes as simple exponential decay

$$G(t)=G_\infty e^{-t/\tau_s}, \tag{3}$$

where the structural decay time, τ_s, is proportional to the solvent viscosity, $\tau_s=\eta/G_\infty$. The resulting VE structural response is also an exponential decay that decays on a slightly longer time scale. Other representative functions have been proposed to model the VE relaxation dynamics,[29,71] but the Maxwell model is the simplest to implement and we used it to analyze our data. The viscoelastic propertics of liquids can be measured with both ultrasound techniques and Brillouin scattering.[71]

The separation of the structural and phonon responses discussed above is an approximation meant to illustrate the physical content of the VE model. In our numerical calculations, we use the exact formulas developed by Berg to simulate the model response functions for comparison with our experimental results.[67] Before beginning our comparison we should note one serious difficulty. The VE model is based on the solvation of a spherical probe molecule, whereas PERY is highly anisotropic with semi axes of approximately 10.5 Å, 6 Å, and 1.5 Å. Thus, direct comparison may be inappropriate. An immediate difficulty arises when calculating the ultrafast phonon response. The VE model predicts that the time scale of this response, τ_{ph}, scales linearly with the solute radius.[67] Unfortunately, PERY's highly anisotropic nature makes identification of the solute radius uncertain. If we estimate an effective radius for PERY to be in the range of $r_c\sim 4-6$ Å (average radius from the total molecular volume), then the predicted ultrafast phonon response occurs on the experimental time scale.

The VE model predicts a pronounced dip in the response within the first 200–400 fs depending on the solute radius. This recurrence, interpreted as a coherent backreaction of the solvent as induced phonons propagate away from the changing cavity, is a prominent characteristic in the VE model. Our data, even in CCl_4, which is the solvent most likely to display pure nonpolar solvation, lack any discernible recurrences (other than the strong vibrational wave packet modulation). However, this lack of observation does not invalidate the VE theory, since the region that the recurrence is predicted to occur is masked by PERY's strong quantum beats. A similar recurrence was observed in a previous 3PEPS study on room temperature PMMA glass, where a critically damped, sub-100 fs oscillation was noticed during the first 200 fs.[50]

In the VE model, the physical picture is that $R(t)$ represents a mechanical response to a size or shape change of the solute following an electronic excitation. This predicted response assumes that the solvent–solute interaction forces are radial as would be expected of nonpolar interactions (e.g., short range repulsive and long range dispersive interactions). This type of response can be considered nonelectrostatic and hence the VE model describes an ideal nonpolar response of the solvent. Even so, we would like to emphasize that though higher order electrostatic interaction forces (quadrupolar–quadrupolar, quadrupolar-induced dipolar) can be approximated as radial forces, Ladanyi and Stratt[72] observed, via

TABLE III. Summary of parameters obtained in viscoelastic calculations.[a]

Solvent	$G_\infty(\times 10^{10})$	$K_\infty(\times 10^{10})$	$K_5(\times 10^{10})$	Radius (Å)
CCl_4	1.5	4.1	2.5	5.9
CS_2	...	...	...	...
Benzene	0.95	3.5	0.9	5.8
Toluene	0.74	5.3	6.8	3.0
Acetonitrile	0.78	4.7	2.0	5.3
Methanol	0.64	1.1	1.4	2.9

[a]Results of the unconstrained fit of the VE response to the simulated $M(t)$ functions presented in Table II. The VE moduli and coupling parameter are in units of dyn/cm^2. All parameters were allowed to float during fit.

instantaneous normal mode (INM) analysis, subtle effects on the relaxation mechanisms in nondipolar systems. These authors observed different, specific solvation mechanisms (relaxation via translational or librational motions) and time scales based principally on the symmetry of the interactions (e.g., a radial Lennard-Jones potential vs an anisotropic quadrupolar–quadrupolar interaction). It is quite plausible that in nondipolar systems, where non-negligible higher order electrostatic moments exist, the nonpolar response predicted in the VE model may be masked by the stronger, higher order electrostatic responses of the solvent.

Since the experimental values for the moduli were not found in the literature, we performed a multiparameter fit of the VE model (Table II) to the simulated $M(t)$ functions.[29] The results of those fits are tabulated in Table III and a comparison of the predicted VE responses and the $M(t)$ functions for benzene and acetonitrile is illustrated in Fig. 5. A similar level of agreement was obtained for the other solvents. As Fig. 5 demonstrates, the VE model, with four arbitrary floating parameters (G_∞, K_∞, K_s, radius), is capable of describing the full relaxation profiles of the solvents (including the polar solvents where the model is assumed not applicable). The values of the parameters used to model the VE response are not unreasonable for such room temperature solvents.[71] The radii found in Table III suggest that the effective radius of PERY to be ~5.5 Å. Even though fixing the radius to 5.5 Å and floating the other VE parameters lead to poorer fits for methanol and toluene, the resulting moduli did not greatly differ, suggesting that the VE model may be less sensitive to the radius than initially expected.

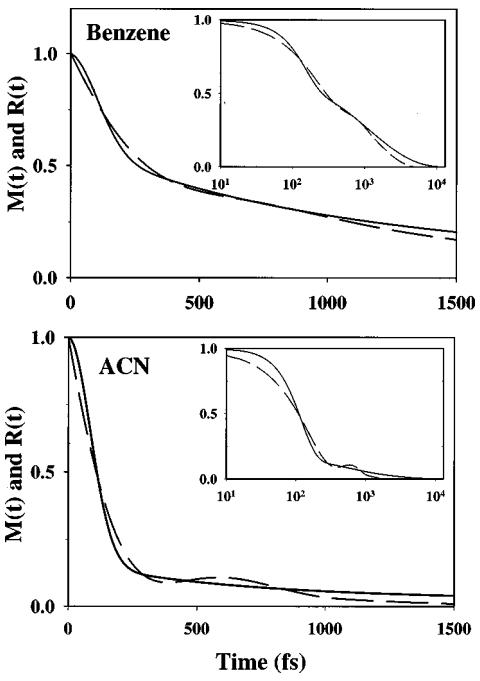

FIG. 5. Comparison of the best fit between the VE responses for benzene (upper panel) and acetonitrile (lower panel). Parameters used are given in Table III. Inset shows the same curves plotted on a log abscissa. Both the solute vibrational and long time component contributions to the experimental data were removed for this comparison.

Berg applied a multicomponent variant of the VE model to describe the solvation dynamics of a hydrated electron.[73] In this work, Berg extended the VE theory to account for arbitrary final cavity shapes, although still maintaining the spherical requirement for the initial cavity. Given the quality of the unconstrained fits in Fig. 5 and our lack of independent knowledge of the required parameters, such an extension does not seem justified in the present case.

B. Other nonpolar solvation investigations

Bagchi and co-workers have used mode coupling theory (MCT) and density functional theory to separate the ultrafast binary component of the interaction from the slow collective contribution, the latter being coupled to the solvent density fluctuations.[43] In their model, they identified an ultrafast component originating from binary collisions that exhibits an ultrafast Gaussian relaxation profile with a time constant of ~100 fs and accounts for ~40%–60% of the total relaxation in studied non-polar systems.[10] These values are in agreement with the theoretical analysis of non-polar electronic transition line shapes.[68–70] In an extension of this theory, Sethia and Bagchi[73] formulated a model to describe the solvation relaxation, arising from the electrostatic interactions, of quadrupole and dipole solutes in a dipolar solvent. They observed that the dipolar solvation occurs more slowly than the quadrupolar solvation and attributed the difference to the coupling of the solute to different length scales of the solvent. Hence, nondipolar solvation processes probe different spatial mechanisms than dipolar solvation and should assist in characterizing the total spatial and temporal dependent solvation response of a liquid.

Skinner and co-workers derived analytical expressions for the solvation correlation functions and absorption profiles of nonpolar chromophores dissolved in nonpolar Lennard-Jones fluids.[68] Their theory includes explicit microscopic considerations such as specific solute–solvent interactions and the solvent structure surrounding the solute. The results of their theory compare favorably with nonpolar simulations,[69,70] and display both short- and long-time behavior that is in qualitative agreement with dynamics observed in our study. Additionally, the predicted temperature dependence of both the solvation correlation function and absorption profile captures many of the features previously observed experimentally by Berg and co-workers.[29–33]

Maroncelli and co-workers have experimentally investigated the nondipolar solvation of a dipolar probe molecule,[1] and showed that for a dipolar solute in polar solvents, the Stokes shift arises predominately from electrostatic interac-

tions between the permanent charge distributions of the solute and solvent. Ladanyi and Maroncelli[17] explored this point further in molecular dynamics simulations and showed that the relative importance of translational motion of solvent molecules increased as the multipolar order of the solute perturbation is increased in both polar (acetonitrile) and nondipolar (CO_2) solvents. These authors investigated the collectivity of the solvation response and found that the solvation in the polar solvent acetonitrile appears more collective in nature, whereas the solvation dynamics in nondipolar carbon dioxide appear to arise from single molecule motions.

Ladanyi and Stratt[72] using INM analysis made a similar point. Their study illustrates that the mechanisms of nonpolar or nondipolar solvation may not depend greatly on the range of the solute–solvent interactions, but rather on the symmetry of the interactions. This suggests that similar mechanisms exist for nonpolar, polar, and nondipolar solvation, but that the role (i.e., magnitude and time scale) of the mechanisms may differ depending on the quickest relaxation route to equilibrium. Kalbfleisch and Zeigler studied the solvation dynamics of CH_3I in Ar with INM, and found a similar time scale and magnitude dependence of the solvent dynamics on the shape of the solute–solvent difference potential between the solute excited and ground states. They found that systems with longer range difference potentials relax more slowly than systems with shorter ranged interactions, suggesting that short range nature of the interactions found in nondipolar systems would manifest themselves in faster dynamical time scales. We did not observe this effect in our study, where similar relaxation time scales in both polar and nondipolar solvents were observed (Table II).

The variations in dipole and quadrupole moments of the chosen solvents shown in Table I suggest that the primary mechanisms of solvation may not be identical in all the solvents. Yet, as the experimental results in Table II demonstrate, the solvation time scales do not change significantly from solvent to solvent. This may imply that either the same mechanisms are at work in all the solvents (whether polar or nondipolar), or more likely, that different mechanisms exist in the different solvents, and they exhibit similar time scales. Despite the similarities in the data, some differences are noticeable. The $\sim$2 ps component found in most solvents (except CS_2) does not appear to be directly correlated with the viscosity of the solvent [e.g., acetonitrile with viscosity of 0.35 cP has a relaxation time comparable to CCl_4 (η=0.97 cP)]. Comparing the data in Table I with the 3PEPS data of Table II, the amplitude of the Gaussian component is significantly larger in the nonpolar solvents with a quadrupolar moment (benzene, toluene) than in CCl_4, which lacks a quadrupole moment. Since PERY is expected to have a sizable quadrupole moment, quadrupole–quadrupole and quadrupole–dipole (for acetonitrile and methanol) may be the dominant interactions in all solvents except in CCl_4, where the quadrupole–octupole interaction would be the dominant electrostatic interaction.

In addition to electrostatic considerations in nondipolar solvation, it may be important to consider the influence of PERY's high polarizability arising from its extended conjugation. Kim and co-workers have recently performed molecular dynamics simulations with polarizable polar solutes dissolved in polar solvents and have shown that the dipole-induced dipole interactions can indeed slow the integrated echo intensity decay in 2PE measurements.[74,75] This effect may not be noticeable in 3PEPS experiments measured with pulses longer than the dephasing time, where the pulses wash out the specific details of the echo decay. However, such polarizability effects may contribute to the nondipolar 3PEPS signals observed here, specifically at short population times ($T<50$ fs), where the integrated echo profiles (Fig. 2) exhibit some asymmetry. Both possible polarizability effects and contributions arising from the weakly coupled interactions are accounted for in the polynomial fitting of the integrated echo profiles. The characterization of the complex interplay between the weak interactions (including higher order permanent electrostatic and induced electrostatic interactions) that may appreciably contribute to solvation dynamics in nondipolar systems poses a difficult problem and requires further investigation, both experimentally and theoretically. For example, comparison of the viscoelastic model with the models described above will require quantitative modeling of the energetics associated with the various interactions.

V. CONCLUDING REMARKS

The 3PEPS technique has allowed accurate extraction of the time scales of nondipolar solvation of a nondipolar solute in a range of solvents at room temperature. With the exception of CS_2, similar time scales are observed regardless of whether the solvent is polar, weakly polar, or nonpolar. In this regard, our results are in qualitative accord with theory,[67] instantaneous normal mode analysis,[72] and simulation studies.[17] It is clear that nondipolar solvation of a nondipolar solute can proceed extremely rapidly with similar time scales to those of the dipolar solvation of a polar solute.

In order to quantitatively interpret our data and provide a microscopic description of the solvation mechanisms in systems such as those studied here, much remains to be done. *Ab initio* calculations of the ground and excited state charge distributions and, if possible geometries of the PERY molecule would allow reliable estimates of the contribution of nonpolar and multipolar solvation contributions. In this regard, a comparison with Reynolds and co-workers' data[1] for a dipolar solute (coumarin 153) in two of the solvents studied here (benzene and toluene) is of interest. In both solvents, they find three relaxation components with the first two being qualitatively similar in time scales and amplitude to those we found for solvation of the nondipolar PERY solute. However, we do not find the small amplitude, slower (15–20 ps) components they reported.

Berg's viscoelastic continuum model can capture the qualitative properties of both nonpolar and polar solvation. Absolute agreement of the model with our experimental data is lacking due to the inaccessibility of necessary input parameters. Further experimental studies are required to confirm the VE model as a predictive model of nonpolar solvation. Further solvation studies with different solutes,

collected over wide temperature ranges are required to clarify the dynamics of weak solute–solvent interactions in liquids.

ACKNOWLEDGMENTS

This work was supported by a grant from the NSF. K.O. is a Japan Society for the Promotion of Science (JSPS) Research Fellow. We would also like to express thanks to Professor Biman Bagchi (Indian Institute of Science) and Professor Mark Maroncelli (Pennsylvania State University) for helpful and informative discussions.

[1] L. Reynolds, J. A. Gardecki, S. J. V. Frankland, M. L. Horng, and M. Maroncelli, J. Phys. Chem. **100**, 10337 (1996).
[2] M. L. Horng, J. A. Gardecki, A. Papazyan, and M. Maroncelli, J. Phys. Chem. **99**, 17311 (1995).
[3] C. F. Chapman, R. S. Fee, and M. Maroncelli, J. Phys. Chem. **99**, 4811 (1995).
[4] P. V. Kumar and M. Maroncelli, J. Chem. Phys. **103**, 3038 (1995).
[5] R. Jimenez, G. R. Fleming, P. V. Kumar, and M. Maroncelli, Nature (London) **369**, 471 (1994).
[6] W. P. de Boeij, M. S. Pshenichnikov, and D. A. Wiersma, Chem. Phys. Lett. **238**, 1 (1995).
[7] W. P. de Boeij, M. S. Pshenichnikov, and D. A. Wiersma, J. Phys. Chem. **100**, 11806 (1996).
[8] W. P. de Boeij, M. S. Pshenichnikov, and D. A. Wiersma, Annu. Rev. Phys. Chem. **49**, 99 (1998).
[9] T. Joo, Y. Jia, and G. R. Fleming, J. Chem. Phys. **102**, 4063 (1995).
[10] T. Joo, Y. Jia, J. Y. Yu, M. J. Lang, and G. R. Fleming, J. Chem. Phys. **104**, 6089 (1996).
[11] M. Cho, G. R. Fleming, S. Saito, I. Ohmine, and R. M. Stratt, J. Chem. Phys. **100**, 6672 (1994).
[12] R. M. Stratt and M. Cho, J. Chem. Phys. **100**, 6700 (1994).
[13] E. W. Castner, Jr. and M. Maroncelli, J. Mol. Liq. **77**, 1 (1998).
[14] J. E. Lewis and M. Maroncelli, Chem. Phys. Lett. **282**, 197 (1998).
[15] S. J. V. Frankland and M. Maroncelli, J. Chem. Phys. **110**, 1687 (1999).
[16] M. Maroncelli, J. Chem. Phys. **94**, 2084 (1991).
[17] B. M. Ladanyi and M. Maroncelli, J. Chem. Phys. **109**, 3204 (1998).
[18] M. Maroncelli, J. Chem. Phys. **106**, 1545 (1997).
[19] S. J. Rosenthal, R. Jimenez, G. R. Fleming, P. V. Kumar, and M. Maroncelli, J. Mol. Liq. **60**, 25 (1994).
[20] M. Maroncelli, J. Mol. Liq. **57**, 1 (1993).
[21] M. Cho, J.-Y. Yu, T. Joo, Y. Nagasawa, S. A. Passino, and G. R. Fleming, J. Phys. Chem. **100**, 11944 (1996).
[22] A. Chandra, D. Q. Wei, and G. N. Patey, J. Chem. Phys. **99**, 2068 (1993).
[23] A. Chandra, D. Q. Wei, and G. N. Patey, J. Chem. Phys. **99**, 4926 (1993).
[24] N. Nandi, S. Roy, and B. Bagchi, Proc.-Indian Acad. Sci., Chem. Sci. **106**, 1297 (1994).
[25] S. Roy and B. Bagchi, J. Chem. Phys. **99**, 9938 (1993).
[26] S. Roy, S. Komath, and B. Bagchi, J. Chem. Phys. **99**, 3139 (1993).
[27] S. Roy and B. Bagchi, J. Chem. Phys. **99**, 1310 (1993).
[28] S. Roy, S. Komath, and B. Bagchi, Proc.-Indian Acad. Sci., Chem. Sci. **105**, 79 (1993).
[29] M. Berg, Chem. Phys. Lett. **228**, 317 (1994).
[30] J. T. Fourkas, A. Benigno, and M. Berg, J. Chem. Phys. **99**, 8552 (1993).
[31] J. T. Fourkas, A. Benigno, and M. Berg, J. Non-Cryst. Solids **172**, 234 (1994).
[32] J. W. Yu, T. J. Kang, and M. Berg, J. Chem. Phys. **94**, 5787 (1991).
[33] T. J. Kang, J. Yu, and M. Berg, Chem. Phys. Lett. **174**, 476 (1990).
[34] T. Fonseca, B. M. Ladanyi, and J. T. Hynes, J. Phys. Chem. **96**, 4085 (1992).
[35] T. Fonseca and B. M. Ladanyi, J. Phys. Chem. **95**, 2116 (1991).
[36] J. Aqvist and T. Hansson, J. Phys. Chem. **100**, 9512 (1996).
[37] F. O. Raineri, Y. Q. Zhou, and H. L. Friedman, Chem. Phys. **152**, 201 (1991).
[38] F. O. Raineri, H. Resat, B. C. Perng, F. Hirata, and H. L. Friedman, J. Chem. Phys. **100**, 1477 (1994).
[39] J. N. Onuchic and P. G. Wolynes, J. Chem. Phys. **98**, 2218 (1993).
[40] G. Goodyear, R. E. Larsen, and R. M. Stratt, Phys. Rev. Lett. **76**, 243 (1996).
[41] R. M. Stratt and M. Maroncelli, J. Phys. Chem. **100**, 12981 (1996).
[42] R. E. Larsen, E. F. David, G. Goodyear, and R. M. Stratt, J. Chem. Phys. **107**, 524 (1997).
[43] R. Biswas, S. Bhattacharyya, and B. Bagchi, J. Chem. Phys. **108**, 4963 (1998).
[44] B. Bagchi, J. Chem. Phys. **100**, 6658 (1994).
[45] R. Mercadante, M. Trsic, J. Duff, and R. Aroca, J. Mol. Struct.: THEOCHEM **394**, 215 (1997).
[46] D. Zimdars, R. S. Francis, C. Ferrante, and M. D. Fayer, J. Chem. Phys. **106**, 7498 (1997).
[47] W. P. de Boeij, M. S. Pshenichnikov, and D. A. Wiersma, Chem. Phys. **233**, 287 (1998).
[48] Y. Nagasawa, J.-Y. Yu, and G. R. Fleming, J. Chem. Phys. **109**, 6175 (1998).
[49] Y. Nagasawa, J.-Y. Yu, M. Cho, and G. R. Fleming, Faraday Discuss. **108**, 23 (1997).
[50] Y. Nagasawa, S. A. Passino, T. Joo, and G. R. Fleming, J. Chem. Phys. **106**, 4840 (1997).
[51] R. Jimenez, F. van Mourik, J.-Y. Yu, and G. R. Fleming, J. Phys. Chem. B **101**, 7350 (1997).
[52] M. L. Groot, J. Y. Yu, R. Agarwal, J. R. Norris, and G. R. Fleming, J. Phys. Chem. B **102**, 5923 (1998).
[53] J.-Y. Yu, Y. Nagasawa, R. van Grondelle, and G. R. Fleming, Chem. Phys. Lett. **280**, 404 (1997).
[54] S. A. Passino, Y. Nagasawa, T. Joo, and G. R. Fleming, J. Phys. Chem. A **101**, 725 (1997).
[55] M. K. Reed, M. K. Steinershepard, and D. K. Negus, Opt. Lett. **19**, 1855 (1994).
[56] M. K. Reed, M. S. Armas, M. K. Steinershepard, and D. K. Negus, Opt. Lett. **20**, 605 (1995).
[57] G. Herzberg, *Atomic Spectra and Atomic Structure* (Prentice–Hall, New York. 1937).
[58] S. A. Hambir, Y. Jiang, and G. J. Blanchard, J. Chem. Phys. **98**, 6075 (1993).
[59] Y. Jiang and G. J. Blanchard, J. Phys. Chem. **98**, 9411 (1994).
[60] A. M. Walsh and R. F. Loring, Chem. Phys. Lett. **186**, 77 (1991).
[61] G. R. Fleming, *Chemical Applications of Ultrafast Spectroscopy* (Oxford University Press, New York, 1986).
[62] S. H. Lee, J. H. Lee, and T. Joo, J. Chem. Phys. **110**, 10969 (1999).
[63] M. Yang, K. Ohta, and G. R. Fleming, J. Chem. Phys. **110**, 10243 (1999).
[64] M. S. Pshenichnikov, K. Duppen, and D. A. Wiersma, Phys. Rev. Lett. **74**, 674 (1995).
[65] J. Gardecki, M. L. Horng, A. Papazyan, and M. Maroncelli, J. Mol. Liq. **65-6**, 49 (1995).
[66] S. Mukamel, *Nonlinear Optical Spectroscopy* (Oxford University Press, New York, 1995).
[67] M. Berg, J. Phys. Chem. A **102**, 17 (1998).
[68] M. D. Stephens, J. G. Saven, and J. L. Skinner, J. Chem. Phys. **106**, 2129 (1997).
[69] S. A. Egorov, N. D. Stephens, and J. L. Skinner, J. Chem. Phys. **107**, 10485 (1997).
[70] J. G. Saven and J. L. Skinner, J. Chem. Phys. **99**, 4391 (1993).
[71] G. Harrison, *The Dynamic Properties of Supercooled Liquids* (Academic, New Francisco, 1976).
[72] B. M. Ladanyi and R. M. Stratt, J. Phys. Chem. **100**, 1266 (1996).
[73] A. Sethia and B. Bagchi, J. Phys. Soc. Jpn. **68**, 303 (1999).
[74] B. D. Bursulaya, D. A. Zichi, and H. J. Kim, J. Phys. Chem. **99**, 10069 (1995).
[75] B. D. Bursulaya, D. A. Zichi, and H. J. Kim, J. Phys. Chem. **100**, 1392 (1996).
[76] *Handbook of Chemistry and Physics*, edited by D. Lide (Chemical Rubber Company, Boston, 1991), Vol. 71.